CBCT Images of Anatomic Landmarks in Maxillofacial Region

Meltem Mayil, Gaye Keser, Filiz Namdar Pekiner

Marmara University, Faculty of Dentistry, Department of Oral Diagnosis and Radiology, Istanbul - Turkey

Yazışma Adresi / Address reprint requests to: Filiz Namdar Pekiner
Marmara University, Faculty of Dentistry, Department of Oral Diagnosis and Radiology, Istanbul - Turkey
Elektronik posta adresi / E-mail address: fpekiner@gmail.com
Kabul tarihi / Date of acceptance: 14 Ağustos 2014 / August 14, 2014

ÖZET

Maksillofasiyal bölgedeki anatomik noktaların CBCT görüntüleri

Diş hekimliği radyolojisinde konvansiyonel çekim teknikleri baş ve boyun bölgesinde üç boyutlu kompleks yapıların sadece iki boyutlu görüntülenmesine olanak verir. CBCT, diğer bir ismiyle dental volumetrik tomografi, maksillofasiyal bölgede daha hızlı veri elde edebilmek amacıyla konvansiyonel bilgisayarlı tomografiye (BT) alternatif olarak geliştirilmiştir. CBCT'nin avantajları arasında daha kısa ışınlama süresi, hasta hareketine bağlı olarak oluşan distorsiyonda azalma, multiplanar görüntüleme olanağı ve hastanın maruz kaldığı dozda azalma bulunmaktadır. CBCT klinisyenlerin maksillofasiyal bölgede yer alan anatomik noktaların lokalizasyonun belirlenmesinde ve anatomik yapıların aksiyal, koronal, sagittal düzlemlerde görüntülenmesine olanak sağlar. Bu derlemede maksillofasiyal bölgede yer alan bazı anatomik noktaların CBCT görüntülerinden bahsetmekteyiz.

Anahtar sözcükler: Anatomik noktalar, CBCT, maksillofasiyal bölge

ABSTRACT

CBCT images of anatomic landmarks in maxillofacial region

Conventional radiographic techniques in dental radiology allows only 2D images of 3D structures of head and neck region. CBCT is a recent technology, is also named as dental volumetric tomography, which was developed as an alternative to conventional CT using cone beam-shaped X-ray to provide more rapid acquisition of a data set of entire maxillofacial region. CBCT has remarkable advantages such as shorter exposure time, reduced image distortion due to patient movements, decreased patient dose and multiplanar screening. CBCT also allows the clinicians to localize the anatomic structures of the maxillofacial region and these anatomic structures can be visualized in various planes such as axial, coronal and sagittal planes. In this review we mentioned some anatomic structures of the maxillofacial region by using CBCT imaging.

Key words: Anatomic landmarks, CBCT, maxillofacial region

INTRODUCTION

Cone beam computed tomography (CBCT) might be one of the most important developments in dental radiology over the years. The first prototype scanner for CBCT was developed and described in 1982 for angiographic applications (1). For dentomaxillofacial use a CBCT scanner was developed in the late 1990s, and since with the first report (2) the CBCT technique has gained great popularity in dentistry. The development has been ast and the name of the technique has varied as cone beam CT, limited cone beam CT, digital volume tomography (DVT), dental volumetric CT and volumetric tomography (3,4).

From the first generations to several new generations on the market has different brand which in the patient is a seated, standing or supine position during the examination.

Imaging is accomplished by using a rotating gantry to which an x-ray source and detector are fixed. A cone-shaped source of ionizing radiation is directed through the middle of the area of interest onto an area x-ray detector on the opposite side. The x-ray source and detector rotate around a rotation fulcrum fixed within the center of the region of interest and only one rotational sequence of the gantry is necessary to acquire enough data for image reconstruction. During the rotation, multiple sequential planar projection images of the field of view (FOV) (from 150 to more than 600) are acquired in a complete, or sometimes partial, arc. This procedure varies from a traditional medical CT, which uses a fan-shaped x-ray beam in a helical progression to acquire individual image slices of the FOV and then stacks the slices to obtain a 3D representation. Each slice requires a separate scan and

separate 2D reconstruction. The next stage is the reconstruction stage and it consists of relating the collected images to each other to create a volumetric data set. This volumetric data set is presented as primary images on the monitor reconstructed in three orthogonal planes (axial, coronal and sagittal) and new reconstructions in all planes, cross-sectional projections at different slice thicknesses are easily performed (3,4).

This technique has several advantages. CBCT volumetric data is isotropic, which means all three dimensions of the image voxels are the same. This makes it possible to reorient the im-ages to fit the patient's anatomic features and perform real-time measurements. Accuracy is another advantage of CBCT. It can generate a size of voxel (a 3D cuboid unit of images) as small as submilimeter in dimension, which contributes to its high resolution and quality. CBCT units provide choices for field of view (FOV), which allows irradiation of particular area of interest to dentists, while limiting irradiation of other tissues. The radiation dose from a CBCT is lower than that from a conventional CT, but is significantly higher than traditional dental radiography techniques. Compared to conventional CT, the compact size and affordability of CBCT makes it suitable for the dental office setting. Moreover, a CBCT image can be reformatted to panoramic, cephalometric, or bilateral multiplanar projections of the temporomandibular joint. In all systems, short scan time allows for quick collection of data from the patient and thus reduces the possibility of motion artifacts. The studies concluded that CBCT technology was useful in maxillofacial radiology, especially for evaluation of hard tissues, although detection and evaluation of soft tissue lesions are not as clear as desired (5-8).

In many circumstances, CBCT is superior to conventional 2D images in demonstrating anatomic structures, the location and extent of pathologies, the quantity and quality of bone, and the spatial relationship of an object relative to the adjacent critical anatomical structures. Applications of CBCT also include impacted mandibular third molar position close proximity to the inferior alveolar canal; determine trace of an impacted canine for orthodontic treatment; orthodontic/surgical management of complex skeletal abnormality; endodontic management of a multirooted tooth when root canal anatomy is not adequately shown on conventional intraoral radiographs; dental trauma (suspected root fracture); implant placement

and fabrication of surgical stents and jaw bone invasion of oral carcinoma. On the contrary, CBCT should not be routinely used for detection of caries, periodontal bone loss, and periapical pathosis or for routine orthodontic diagnosis (6,9). The purpose of this review was to identify anatomic structures of mandible and maxilla that were assessed with CBCT.

Inferior Mandibular Canal

The location of the inferior mandibular canal (IMC) is a critical factor that can influence dental implant or impacted third molar surgery. In addition this, IMC may also be damaged by osteotomies or fracture repair; thus, a strong understanding of the intrabony anatomy of the mandibular canal is required before conducting dental implant surgery or other operative procedures. However, distortion of 2D panoramic radiography often results in miscalculation of the IMC location (10,11). It is recommended that CBCT, especially cross-sectional imaging offers an excellent image of the morphology of the mandible and the exact location of the IMC, reporting that a defined canal can be detected on the majority of the images (12-14). IMC is tube-like structure that transverses whole length of mandible from the mandibular foramen in the ramus till the mental foramen in the premolar region (Figure 1). On a CBCT image it appears like a radiolucent circle surrounded by thin radiopaque ring which represents the wall of the canal. This canal is best visible on coronal and cross-sectional images and it is difficult to visualize on axial slices. On sagittal views the canal might take a variable tube like appearance depending on the actual location and orientation of the slice selected (15).

Mental Foramen

The mental foramen (MF) is an opening on the external surface of the mandible which is typically located in the premolar region and it signifies the anterior end of the IMC and it possess the mental nerve and vascular supply to lowerlip region. Radiographically it appears a crescent incomplete circle which is readily visible on each of three orthographic views (15) (Figure 1).

One of the most challenged regions for implantation in mandible is MF region. This is because there are many
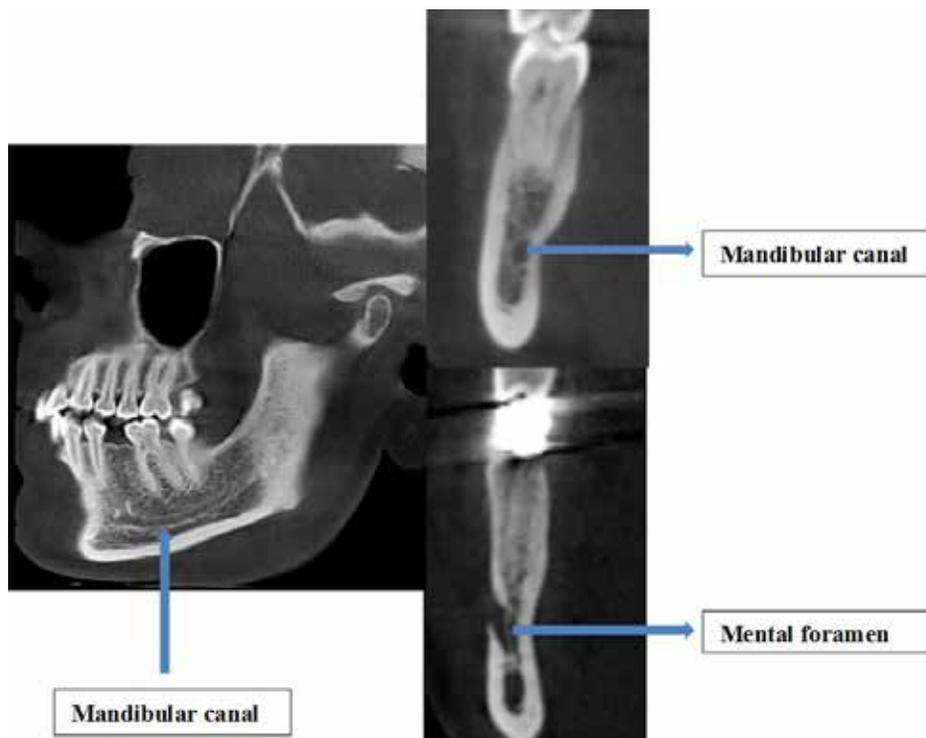
Figure 1: The mandibular canal, mental foramen are seen on sagittal and cross-sectional views

variations with regards to the size, shape, location and direction of the opening of the MF. The shape of MF can be round or oval: diameter changes. The location of MF differs in the horizontal and vertical planes. The most popular method for the identification of MF in the horizontal plane was proposed by Green (16). In this method, the position of MF was recorded as either in the line with the longitudinal axis of a tooth or as lying between the two teeth. It was shown in number of studies that the location of MF is related also with race (17,18). When planning dental implant operation, clinicians should identify vertical MF position, because after the extraction of teeth and due to resorption of alveolar bone, the MF is closer to the alveolar crest. In extreme degrees of resorption, the mental nerve and the final part of inferior alveolar nerve were found directly under the oral mucosa.

In some instance there can be an accessory MF. Katakami et al. (21) diagnosed 17 accessory foramina in 16 patients using limited CBCT for 150 patients. Similarly, Naitoh et al. (22) studied 157 patients CBCT images and found the accessory MF observed in 7% of patients. Accessory MF tended to exist in the apical area of the first molar and posterior or inferior area of the MF. The accessory branches

of the mandibular canal showed common characteristics in the course of gently sloping posterosuperior direction in the buccal surface area.

The IMC may also extend beyond the mental foramen as an intraosseous anterior loop. As reported by Bavitzet (19) and Misch (20) more precise description is: "where the mental neurovascular bundle crosses anterior to the mental foramen than doubles back to exit the mental foramen". The location of foramen, as well as, the possibility that an anterior loop of the mental nerve may be present mesial to the mental foramen need to be detected with CBCT before the surgery to avoid mental nerve injury.

Mandibular Condyle and Coronoid Process

It is essential to obtain a clear and precise image of the temporomandibular joint (TMJ) region. This may be difficult owing to the superimposition of adjacent structures, different angulations of the condyle, limitation of mouth opening in some patients, presence of artifacts and mandibular movements during the examination (23). The TMJ can be viewed using panoramic and transcranial radiographs, conventional CT, CBCT, MRI and arthrography.
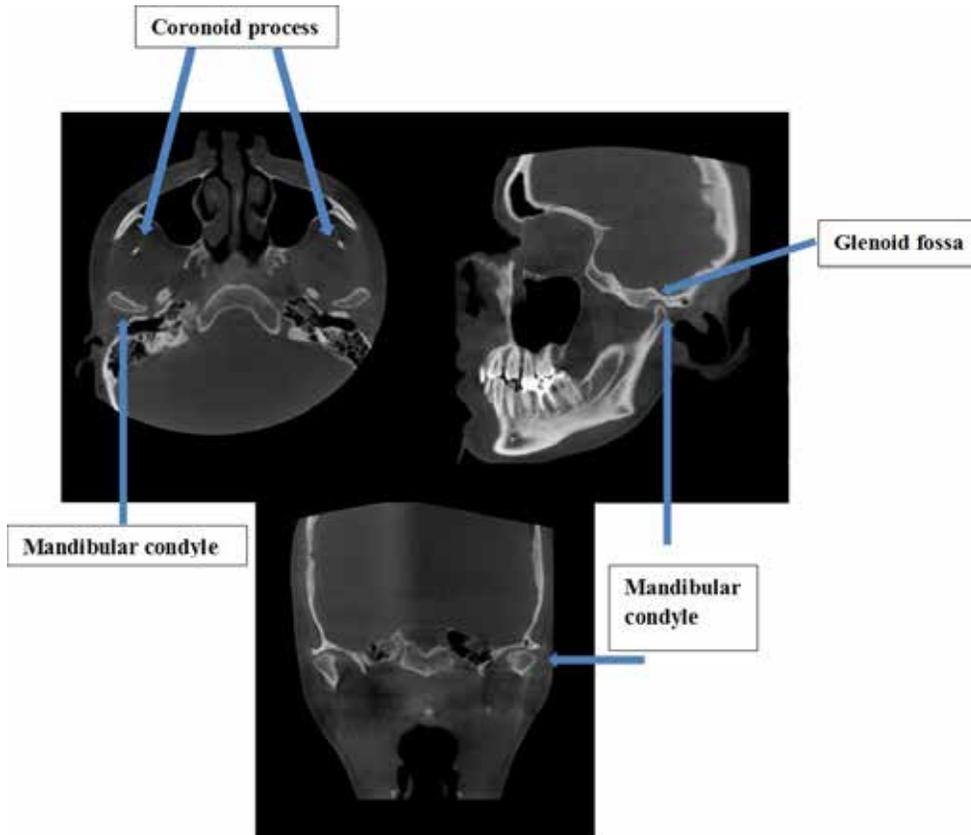
Figure 2: Temporomandibular joints are seen on coronal, sagittal and axial views

CT has been the method of choice to assess the contours of the cortical bone and TMJ dynamics. However, it is a high-cost examination and requires a high dose of radiation (24). Due to the several advantages mentioned before CBCT is favoured and provides a complete radiographic investigation of the bony components of the TMJ. The reconstructed cross-sectional views images of TMJ region or images reconstructed on TMJ tool are high diagnostic quality. CBCT has been shown to be efficient in the diagnosis of several bone changes that affect the TMJ (25,26).

The head of the condyle is an elliptical shaped bony process which serves as the articulation site of the mandible with the temporal bone at the TMJ region. The articulation surface of condyle is hemicylindrical antero-posteriorly. Typically, on both of the sagittal and coronal sections, the hemicylindrical shape of the condylar head can be observed while on the axial sections the elliptical appearance is more prominent. On the coronal view in the open-mouth situation, it often leads to a clearer view of the condyle, since it translates slightly over the tubercle giving an

unobstructed view of the condyle head (Figure 2). Also the coronoid process is a thin bony prominence located in the anterior superior portion of the ramus mandible which is flattened lateromedially. It serves as the attachment site for the muscles of the mastication and on its medial surface is the attachment point of the temporalis muscle. On CBCT it appears like a prolonged elongation that is continuous with that of the mandibular ramus on both of the sagittal and the coronal views while it demonstrates a triangular shape on corresponding axial slice (15,26) (Figure 2).

Mandibular Incisive Canal and Lingual Foramen

The mandibular incisive canal (MIC) is described as a continuation of the IMC and contains one of the terminal branches of the inferior alveolar nerve. The MIC is mostly shown as a tube-like structure and a prolongation of the IMC anterior to the mental foramen, continues towards the incisor region in a slightly downward direction, narrowing crossing the midline and sometimes it reaches only the
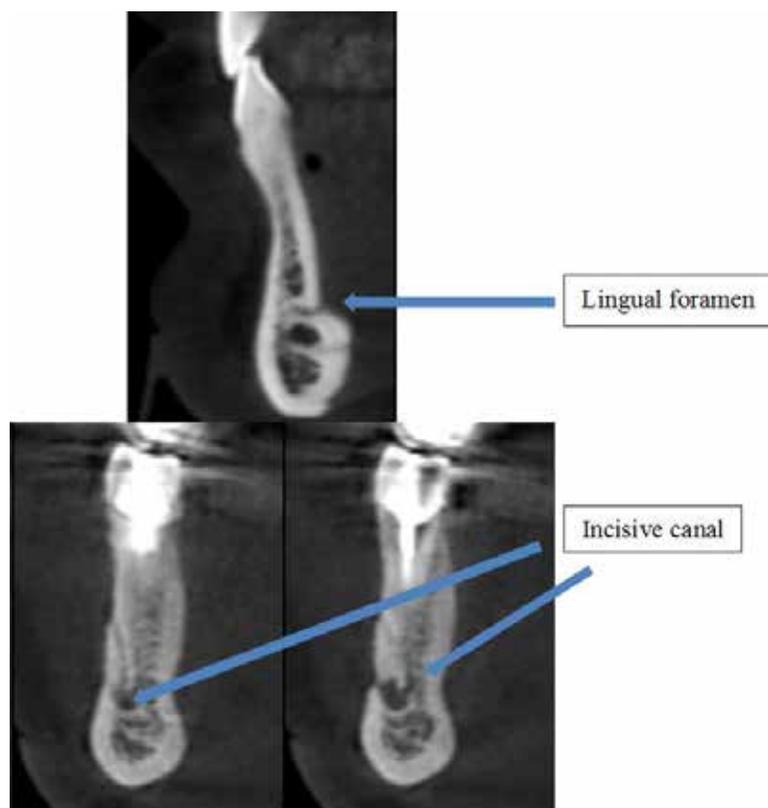
Figure 3: The lingual foramen and mandibular incisive canal are seen on cross-sectional views

midline (27) (Figure 3). The lingual foramen (LF) is usually situated in the internal region of the mandibular symphysis and begins superior to the mental spines and contains an artery that develops from the anastomosis of the two sublingual arteries and ends at the buccal lingual cortex (28). The importance of these observations could be significant, as several surgical procedures are performed in this region. In case of large MIC, a patient may experience discomfort during osteotomy or experience postoperative pain that requires no implant insertion or implant removal (30).

The conventional two-dimensional presurgical radiological assessment often fails to show these structures (30). Contemporary imaging techniques such as CBCT may be particularly suitable in the preoperative treatment planning. The MIC and LF is best seen in cross-sectional views (31) (Figure 3).

Frontal Sinus

The frontal sinus (FS), an air filled cavity, is located in the forehead region just superior to the paired nasal bones. The sinus is usually two in number which are seldom symmetrical (32). For the development of the facial skeleton FS is "an epiphyseal platform" (33). The anterior wall thickness is inversely correlated with FS dimensions and a bony septum separates two cavities, yet variations do exist. Radiographically, the shape of the FS is variable yet readily visible on three orthographic views. It is a radiolucent cavity surrounded by thick cortical layer of the frontal bone (Figure 4 and 5).

Orbita

The medial wall of the orbital cavity or "orbit" is formed by the frontal process of maxilla and the ethmoidal bone. The floor is formed by the orbital process of the maxilla and the zygomatic bone laterally. The zygomatic bone forms also the lateral wall of the orbit in conjunction with the frontal bone which also constitutes the roof of the orbit. The orbital cavity is readily visible as a large round or oval radiolucent cavity and it is best visualized on the coronal slices of CBCT (15) (Figure 4).
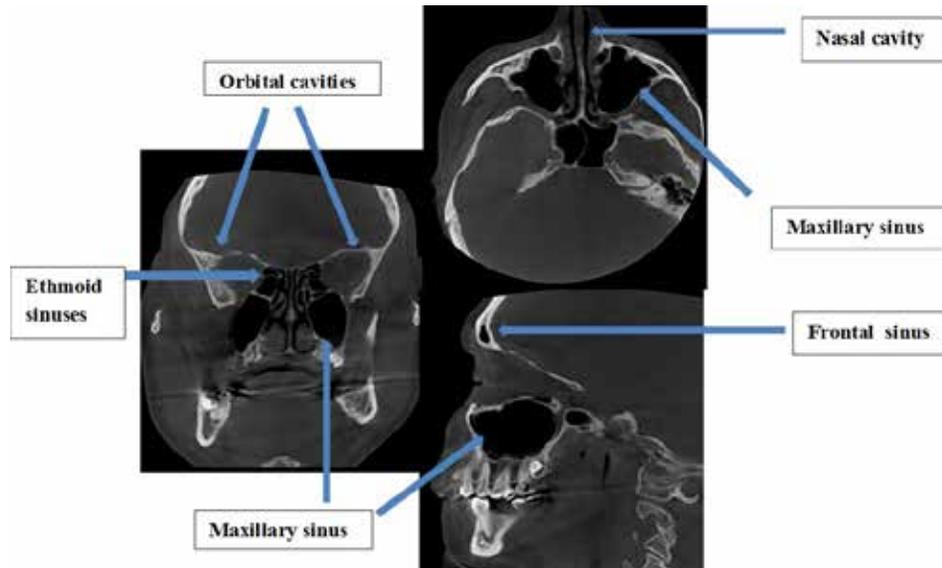
Figure 4: The maxillary, frontal sinus, orbital and nasal cavities are seen on coronal, axial, sagitaal views

Nasal Cavity

It is a pear-shaped cavity which is bounded by the maxillary sinus laterally and the ethmoidal sinus superiorly. It is separated into three distinct chambers (meati or turbinates) on either side of three osseous processes, the nasal conchae (inferior, middle, and superior) (34). Posteriorly, it communicates with the oro-pharynx while inferiorly it communicates with the oral cavity through the naso-palatine duct or canal. It appears as a large, pear-shaped cavity on the coronal slices in CBCT while on the axial and sagittal slices, the cavity should be traced along the path of the nasal concha and the middle nasal septum (Figure 4 and 5).

Nasal Septum

The nasal septum is a mid-sagittal septa that divides the nose into two compartments, it is composed of hard tissue (vomer) and soft tissue (nasal cartilage). Vomer is a thin,
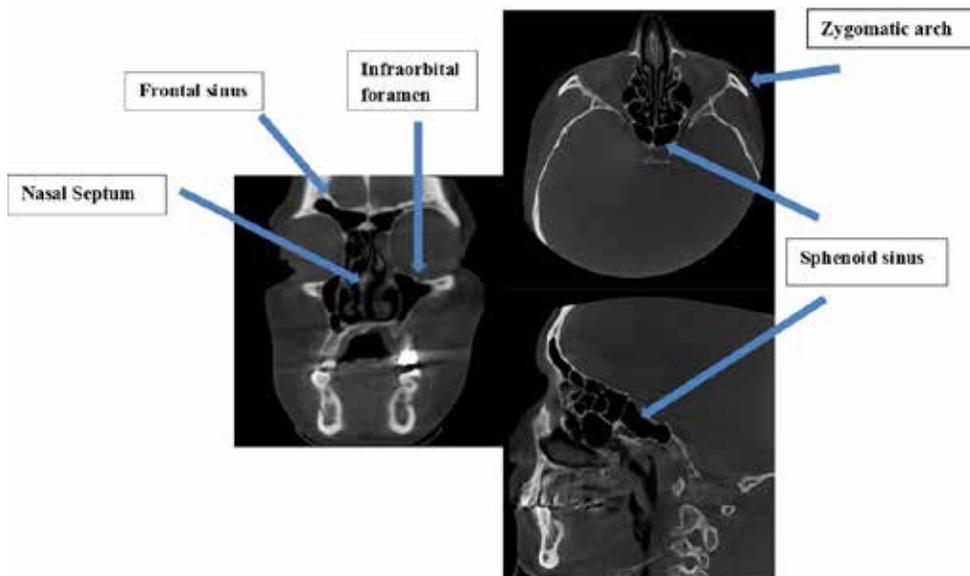
Figure 5: The maxillary, frontal, sphenoid sinuses, nasal septum and also infraorbital foramen are seen on sagittal, coronal and axial views

quadrilateral shaped structure and which the lower part of the nasal septum (35). Radiographically, it is readily visible on the coronal sections as a longitudinal line segmenting the nasal cavity and on the mid-saggital plane, the anterior soft tissue cartilage and the posterior hard tissue bone can be visualized. On trans-axial slices, it runs along the nasal cavity antero-posteriorly while surrounded by the nasal concha anteriorly and the ethmoidal sinuses in the posterior region (Figure 4 and 5).

Sphenoid Sinus

Because of its isolated location and inaccessibility, it is a highly overlooked structure, which is located deep in the nasal cavity. The access to the sphenoid sinus (SS) by physical examination is not very easy, and it cannot be visualized even by routine radiological studies (36,37). By the help of imaging techniques such as CT and MRI, the anatomy of the sphenoid sinus became more important due to its close proximity to highly important structures. The SS is located on the midline and it separates the anterior and middle cranial fossa from each other (38). This cavity that is filled with air and separated by a bony septum and is adjacent to vital structures such as the internal carotid artery (39). Radiographically healthy sphenoid sinus appearance is dark/black and is located just posterior to the ethmoid sinuses and below the base of sphenoid bone (34) (Figure 5).

Ethmoid Sinus

The ethmoid sinuses (ES) are present at birth and enlargement of the sinus terminates by age of 12 (40). The ES are made up of multiple, small air cells separated by the vomer bone in the midline. Due to the complicated anatomy of the sinus, it can also be portrayed as "ethmoid labyrinth" (34) (Figure 4 and 5).

Originated from pneumatization of the bone plate, concha bullosa is a variation which is actually the extension of the ethmoid cells. It may be either uni or bilateral. Varied degrees of pneumatization of the concha may be observed, possibly causing middle meatus or infundibulum obstruction.

The ethmoid cells those are located at posterior region may reach the posterior ethmoid capsule or move to the medial aspect of the optic nerve. These are named as Onodi cells (spheno-ethmoid cells which are positioned between the sphenoid sinus and the floor of the anterior cranial fossa (33).

The largest air cell of the ethmoid labyrinth is the ethmoid bulla. When this air cell reaches sufficient size it can tighten or even obstruct the middle nasal meatus and the infundibulum.

In a study conducted it is reported that the prevalence of ethmoid bulla is 8% (41).

Maxillary Sinus

The maxillary sinus (MS) is a pyramidal shaped cavity and it is filled with air. The base of the pyramid is situated medially toward the nasal cavity with which the MS communicates through the ostium and a bony septum may be visible in the sinus floor (Underwood septum) (42). Radiographically, the sinus can be easily seen in all of the 3 orthographic views as a large triangular, radiolucent compartment surrounded by cortical bone (Figure 4). The MS is lined by a mucosal layer that appears on the radiograph as a thin lining to the cavity; in case of infection, this mucosal layer is typically thickened and increased in size.

Infraorbital Foramen

Infraorbital margin is formed laterally by zygomatic bone, medially by maxilla. About 1cm below the infraorbital (IF) margin is the infraorbital foramen for the passage of infraorbital vessels and nerve (43). It is also the facial opening of the infraorbital canal extending from the pterygo-palatine fossa from behind the maxillary tuberosity and reaches through the floor of the orbit to end up. The IF appears as a round radiolucent opening situated in the superior border of the maxillary sinus lateral to the nasal cavity (Figure 5).

Zygomatic Bone

The zygomatic bone is a pyramidal bone which forms the lateral wall of the orbit and with the zygomatic process of the temporal bone it forms the zygomatic arch. It is a strong buttress of lateral portion of middle third of facial skeleton and is responsible for midface contour and

protection of orbital contents (44,45). Zygoma plays a major role in facial contour, and any damage of zygomatic bone carries a risk of functional and aesthetic deficiency (46,47). Radiographically, on the coronal sectional slices, the bone might appear constricted in the middle due to presence of the zygomaticofacial canal (Figure 5).

Anterior Nasal Spine

Anterior nasal spine represents the anterior most end of the nasal cavity and it is formed by the union of the paired maxillary bones. Radiographically, it exhibits a triangular shaped spine on cross-sectional views (15) (Figure 6).

Figure 6: The anterior nasal spine is seen on cross-sectional view

REFERENCES

1. Robb R. Dynamic spatial reconstructor: an x-ray video fluoroscopic CT scanner for dynamic volume imaging of moving organs. IEEE Trans Med Imaging. 1982;1:22-23.

2. Mozzo P, Procacci C, Tacconi A, Martini PT, Andreis IA. A new volumetric CT machine for dental imaging based on the cone-beam technique: preliminary results. Eur Radiol. 1998;8:1558-1564.

3. Scarfe WC, Farman AG. What is cone-beam CT and how does it work? Dent Clin North Am. 2008;52:707-730.

4. Miracle AC, Mukherji SK. Conebeam CT of the Head and Neck, Part 1: Physical Principles AJNR Am J Neuroradiol. 2009;30:1088-1095.

5. MacDonald-Jankowski DS, Orpe EC. Some current legal issues that may affect oral and maxillofacial radiology. Part 2: digital monitors and cone-beam computed tomography. J Can Dent Assoc. 2007;73:507-511.

6. Valentin J. The 2007 recommendation of the International Commission on Radiological Protection, publication 103. Ann ICRP. 2007;37:1-332.

7. Carter L, Farman AG, Geist J, Scarfe WC, Angelopoulos C, Nair MK, Hildebolt CF, Tyndall D, Shrout M. American Academy of Oral Maxillofacial Radiology executive opinion statement on performing and interpreting diagnostic cone beam computed tomography. Oral Surg Oral Med Oral Pathol Oral Radiol Endod. 2008;106:561-562.

8. Razavi T, Palmer RD, Davies J, Wilson R, Palmer PJ. Accuracy of measuring the cortical bone thickness adjacent to dental implants using cone beam computed tomography. Clin Oral Implants Res. 2010;23:718-725.

9. Adibi S, Zhang W, Servos T, O'Neill PN. Cone Beam Computed Tomography in Dentistry: What Dental Educators and Learners Should Know. J Dent Educ. 2009;76:1437-1442.

10. Serhal CB, Jacobs R, Flygare L, Quirynen M, Van Steenberghe D. Perioperative validation of localisation of the mental foramen. Dentomaxillofac Radiol. 2002;31:39-43.

11. Yang J, Cavalcanti MGP, Ruprecht A, Vannier MW. 2-D and 3-D reconstructions of spiral computed tomography in localization of the inferior alveolar canal for dental implants. Oral Surg Oral Med Oral Pathol Oral Radiol Endod. 1999;87:369-374.

12. Nakagawa Y, Kobayashi K, Ishii H, Mishima A, Ishii H, Asada K, Ishibashi K. Preoperative application of limited cone beam computerized tomography as an assessment tool before minor oral surgery. Int J Oral Maxillofac Surg. 2002;31:322-326.

13. Ito K, Gomi Y, Sato S, Arai Y, Shinoda K. Clinical application of a new compact CT system to assess 3-D images for the preoperative treatment planning of implants in the posterior mandible A case report. Clin Oral Implants Res. 2001;12:539-542.

14. Kamburoglu K, Kilicx C, Ozen T, Yuksel SP. Measurements of mandibular canal region obtained by conebeam computed tomography: A cadaveric study. Oral Surg Oral Med Oral Pathol Oral Radiol Endod. 2009;107:34-42.

15. Maxillofacial Radiology Cone Beam CT Interactive Learning And Navigation. Avaliable from: http://www.marcilan.com/anatomy/mpr/

16. Green RM. The position of the mental foramen: a comparison between the southern (Hong Kong) Chinese and other ethnic and racial groups. Oral Surg Oral Med Oral Pathol. 1987;63:287-290.

17. Neiva RF, Gapski R, Wang HL. Morphometric analysis of implant-related anatomy in Caucasian skulls. J Periodontol. 2004;75:1061-1067.

18. Apinhasmit W, Chompoopong S, Methathrathip D, Sansuk R, Phetphunphiphat W. Supraorbital Notch/Foramen, Infraorbital Foramen and Mental Foramen in Thais: anthropometric measurements and surgical relevance. J Med Assoc Thai. 2006;89:675-682.

19. Bavitz JB, Harn SD, Hansen CA, Lang M. An anatomical study of mental neurovascular bundle – implant relationship. Int J Oral Maxillofac Implants. 1993;8:563-567.

20. Misch CE, Crawford EA. Predictable mandibular nerve location. A clinical zone of safety. Int J Oral Implantol. 1990;7:37-40.

21. Katakami K, Mishima A, Shiozaki K, Shimoda S, Hamada Y, Kobayashi K. Characteristics of accessory mental foramina observed on limited cone-beam computed tomography images. J Endod. 2008;34:1441-1445.

22. Naitoh M, Hiraiwa Y, Aimiya H, Gotoh K, Ariji E. Accessory mental foramen assessment using cone-beam computed tomography. Oral Surg Oral Med Oral Pathol Oral Radiol Endod. 2009;107:289-294.

23. Lascala CA, Panella J, Marques MM. Analysis of the accuracy of linear measurements obtained by cone beam computed tomography. Dentomaxillofac Radiol. 2004;33:291-294.

24. Brooks SL, Brand JW, Gibbs SJ, Hollender L, Lurie AG, Omnell KA, Westesson PL, White SC. Imaging of the temporomandibular joint: a position paper of the American Academy of Oral and Maxillofacial Radiology. Oral Surg Oral Med Oral Pathol Oral Radiol Endod. 1997;83:609-618.

25. Hintze H, Wiese M, Wenzel A. Cone beam and conventional tomography for the detection of morphological temporomandibular joint changes. Dentomaxillofac Radiol. 2007; 36:192-197.

26. Tsiklakis K, Syriopoulos K, Stamatakis HC. Radiographic examination of the temporomandibular joint using cone beam computed tomography. Dentomaxillofac Radiol 2004;33:196-201.

27. Olivier E. The inferior dental canal and its nerve in the adult. Br Dent J. 1928;49;356-358.

28. McDonnell, D, Reza Nouri, M, Todd M.E. The mandibular lingual foramen: a consistent arterial foramen in the middle of the mandible. J Anat. 1994;184:363-369.

29. Kohavi D, Bar-Ziv J. Atypical incisive nerve: clinical report. Implant Dent. 1996;5:281-283.

30. Mardinger O, Chaushu G, Arensburg B, Taicher S, Kaffe I. Anterior loop of the mental canal: an anatomical-radiologic study. Implant Dent. 2000;9:120-125.

31. Makris N, Stamatakis H, Syriopoulos K, Tsiklakis K, Stelt PF. Evaluation of the visibility and the course of the mandibular incisive canal and the lingual foramen using cone-beam computed tomography. Clin Oral Impl Res. 2010;21:766-771.

32. Pondé JM, Andrade RN, Vıa JM, Metzger P,Teles AC. Anatomical Variations Of The Frontal Sinus. Int J Morphol. 2008;26:803-808.

33. Pekiner F. Anatomic Variations of Paranasal Sinus on Multidetector Computed Tomography Examinations for Functional Endoscopic Sinus Surgery. MÜSBED 2013;3:102-106.

34. Angelopoulos C. Cone Beam Tomographic Imaging Anatomy of the Maxillofacial Region. Dent Clin N Am. 2008;52: 731-752.

35. Gray H. Anatomy of the Human Body. Philadelphia: Lea & Febiger, 1918; Bartleby.com, 2000. www.bartleby.com/107/.

36. Nour YA, Al-Madani A, El-Daly A, Gaafar A. Isolated Sphenoid Sinus Patology: Spectrum of Diagnostic and Treatment Modalities. Auris Nasus Larynx. 2008;35:500-508.

37. Kazkayası M, Karadeniz Y, Arıkan OK. Anatomic Variations of the Sphenoid Sinus on Computed Tomography. Rhinology. 2005;43:109-114.

38. Budu V, Mogoantă CA, Fănuţă B, Bulescu I. The anatomical relations of the sphenoid sinus and their implications in sphenoid endoscopic surgery. Rom J Morphol Embryol. 2013; 54:13-16.

39. Saka C, Sonbay D, Akın İ, Şimşek G, Öztürk H. Newly Defined Sphenoid Variation That Can Cause Surgical Insufficiency: Sphenoseptal Cell (Sphenoseptal Cell). J Clin Anal Med. 2012;3:18-20.

40. Dwivedi AND, Singha KK. CT Of The Paranasal Sinuses: Normal Anatomy, Varıants And Pathology. Journal of Optoelectronics and Biomedical Materials. 2010;4:28-289.

41. Zinreich XJ. Imaging of the nasal cavity and paranasal sinuses. Curr Opin Radiol. 1992;4: 112-116.

42. Abrahams JJ, Hayt MW, Rock R. Sinus lift procedure of the maxilla in patients with inadequate bone for dental implants: radiographic appearance. Am J Roentgenol. 2000; 174:1289-1292.

43. Lokanayaki V. Anatomic Variations Of Infra Orbital Foramen. Journal of Surgery. 2013;2:30-36.

44. Covington DS, Wainwright DJ, Teichgrarber JF. Changing patter in epidemiology and treatment of zygoma fractures, 10 year review. J Trauma. 1994;27:243-247.

45. Jansma J, Bos RR, Vissink A. Zygomatic fractures. Ned Tijdschr Tandheelkd. 1997;104:436-439.

46. Wahab N, Mehdi H, Khan M. Causes of Zygomatic bone fracture reported at Mayo Hospital, Lahore. J Pak Dent Assoc. 2008;17:31-34.

47. Lee KH, Antoun J. Zygomatic fractures presenting to a tertiary trauma centre, 1996-2006. N Z Dent J. 2009;105:4-7.